ISSN 1066-369X, Russian Mathematics, 2023, Vol. 67, No. 11, pp. 34–48. © Allerton Press, Inc., 2023.
Russian Text © The Author(s), 2023, published in Izvestiya Vysshikh Uchebnykh Zavedenii. Matematika, 2023, No. 11, pp. 41–58.

Method and Algorithm for Calculating Isobaric and Nonisobaric Three-Dimensional Turbulent Jets of Reacting Gases

S. Khodzhiev[a,*,**]

[a] *Bukhara State University, Bukhara, 200100 Republic of Uzbekistan*

**e-mail: Safar1951@yandex.ru*

***e-mail: s.hojiev@buxdu.uz*

Received March 29, 2023; revised May 9, 2023; accepted May 29, 2023

Abstract—This paper presents a calculation method and algorithm, as well as numerical results of studying chemically reacting turbulent jets based on three-dimensional parabolic systems of Navier–Stokes equations for multicomponent gas mixtures. Continuity equations are used to calculate the mass imbalance when solving with constant pressure, and with variable pressures, with the equations of motion and continuity. Diffusion combustion of a propane–butane mixture flowing from a square-shaped nozzle in a submerged flow of an air oxidizer is numerically studied. Pressure variability significantly affects the velocity (temperature) profiles in the initial sections of the jet, and, when moving away from the nozzle exit, the pressure effect can be considered imperceptible, but the plume length is longer than that at constant pressure, but it does not significantly affect the shape of the plume. The saddle-shaped behavior of the longitudinal velocity in the direction of the major axis is numerically obtained for large initial values of the turbulence kinetic energy of the main jet. The presented method allows studying nonreacting and reactive turbulent jets flowing from a rectangular nozzle.

Keywords: jet, three-dimensionality, Navier–Stokes equations, parabolic, model, turbulence, displacements, growth, diffusion combustion, isobaric, nonisobaric, plume, imbalance

DOI: 10.3103/S1066369X23110038

INTRODUCTION

Flow processes such as combustion theory, gas dynamics of lasers, chemical technology in internal combustion engines, rocket engines, and a number of other processes are described by a complex system of nonlinear second-order partial differential equations that take into account the interaction of gas flow and chemical processes. Currently, it is impossible to imagine the development of modern science without the widespread use of mathematical modeling.

An indispensable effective method for theoretical study of flows of chemically reacting media is numerical modeling. This method is currently being intensively developed by improving efficient computational algorithms and conducting numerous computational experiments [1–4].

The most common method of building models is to apply the fundamental laws of nature to a specific situation, such as energy conservation and conservation of matter and momentum [1, 2].

Especially, three-dimensional boundary jet flows have become the subject of experimental and theoretical studies in recent years [5]. The study of methods for calculating three-dimensional turbulent flows is difficult due to the lack of any satisfactory turbulence model for three-dimensional flows. Therefore, progress in various fields of technology and science requires the development of effective methods for calculating a three-dimensional turbulent boundary layer and a jet with chemical reactions [1, 2].

In the applied gas dynamics of reacting jet flows, studies of the propagation of jets flowing from a rectangular channel are of considerable interest. Firstly, such flows are very widely used in technology, such as combustion chambers of gas turbines, the creation of combustion units, the spread of air from a ventilation pipe, and the emission of harmful substances in the atmosphere. Secondly, they represent a solution to the scientific-theoretical problem of a flow moving in a cocurrent flow, which does not belong to the class of problems in the boundary layer theory. In [6–11] and other experimental works, free jets flowing from a rectangular nozzle were considered. The main studies are devoted to finding the trajectory of the jet using various assumptions and do not provide data on the initial distribution of the velocity component

and dynamic characteristics of the flow at the nozzle exit, which significantly affect the propagation of the jet and the parameters of the plume during combustion.

To analyze combustion processes in cocurrent flows numerically, we need the dependences between the geometric characteristics of the flow and the physical parameters of the flows at the inlet and the channel geometry.

Of particular interest is the area of parameters of the outflow of reacting gas mixtures from a rectangular nozzle with a finite aspect ratio into a cocurrent flow, which has great practical application, but has been little studied. The complexity of solving such a problem is associated with a number of difficulties: three-dimensionality, incompleteness of the theory of turbulence and a mathematical model based on the peculiarities of the hydroaerodynamic equations, such as nonlinearity, high order (especially in relation to three-dimensional problems), as well as the insufficiency of effective computational methods.

The final analysis of a symposium held in West Berlin in 1982 by the International Union of Pure and Applied Mechanics on the current state of the problem of three-dimensional boundary layer research provides conclusions about the difficulties of experimental and computational studies of three-dimensional flows.

An important conclusion of the research is that turbulence models based on the concept of isotropic turbulent viscosity require significant improvement in the calculation of three-dimensional turbulent flow.

All participants in the discussion agreed that there is no universal model of turbulence, and over the next ten years, turbulence researchers will have to abandon currently known algorithms, since by then they will have access to new generation computers [5]. There is a need for a better theoretical justification of the mathematical side of this problem and a wider use of simple calculation methods and modern powerful computing tools [12].

1. GOAL AND PROBLEM FORMULATIONS

This work is aimed at selecting a mathematical model to describe three-dimensional turbulent jets of reacting gas mixtures flowing from a rectangular nozzle with a finite ratio of side lengths 2a and 2b into a cocurrent jet during diffusion combustion and at developing effective numerical methods for studying the process.

Note that, in order to calculate turbulent flows, it is necessary to accept the closure hypothesis for apparent turbulent stresses and heat flows [13]. It is important to remember that turbulence models must be validated by comparing calculations based on them with experimental data.

The initial stage of jet flows, including combustion, is directly related to algebraic models of turbulence, which are built on the basis of the Boussinesq hypothesis about turbulence. One of the most successful models of this type is the Prandtl model.

For three-dimensional shear layers, the Prandtl formula usually has the form [5, 13]

$$\mu_T = \rho l^2 \sqrt{\left[\left(\frac{\partial u}{\partial y}\right)^2 + \left(\frac{\partial \omega}{\partial y}\right)^2\right]},$$

where l is the mixing path length.

This model gives qualitatively correct results for near-wall flows. Algebraic models have proven themselves well for relatively simple fluid flows, but require modification to calculate more complex flows, such as reacting jets with combustion.

To date, numerous turbulence models have been proposed, both with one ordinary differential equation, with one partial differential equation and one ordinary differential equation, and models with two partial differential equations, as well as higher order ones, etc. One of the most often used models with two equations is (k–ε)-model.

In this work, as the first option for calculating turbulent viscosity, we use a modified algebraic model that takes into account molecular transport, three-dimensionality, and temperature inhomogeneity of the jet in the form [14]

$$\mu_T = \mu_1 + \varkappa \rho l^2(y,z)\sqrt{\left(\frac{\partial u}{L\partial y}\right)^2 + \left(\frac{\partial u}{\partial z}\right)^2 + \left(\frac{\partial \omega}{L\partial y}\right)^2}\left(\frac{T}{T_2}\right)^{\alpha}. \quad (1)$$

Here, μ_l is the dynamic coefficient of laminar viscosity, $\varkappa$ is the empirical turbulence constant, $l(y,z)$ is the displacement path length, α is the parameter taking into account temperature heterogeneity, and T_2 is the temperature on the axis of the main jet.

In the second option, we use the equations of kinetic and dissipation of kinetic energy of turbulence to calculate turbulent viscosity, having the following form [14, 15]:

$$\rho u\frac{\partial k}{\partial x}+\rho\vartheta\frac{\partial k}{L\partial y}+\rho\omega\frac{\partial k}{\partial z}=\frac{1}{L^2}\frac{\partial}{\partial y}\left(\frac{\mu_{\mathrm{T}}}{\sigma_K}\frac{\partial k}{\partial y}\right)+\frac{\partial}{\partial z}\left(\frac{\mu_{\mathrm{T}}}{\sigma_K}\frac{\partial k}{\partial z}\right)+G-\rho\varepsilon, \tag{2}$$

$$\rho u\frac{\partial \varepsilon}{\partial x}+\rho\vartheta\frac{\partial \varepsilon}{L\partial y}+\rho\omega\frac{\partial \varepsilon}{\partial z}=\frac{1}{L^2}\frac{\partial}{\partial y}\left(\frac{\mu_{\mathrm{T}}}{\sigma_\varepsilon}\frac{\partial \varepsilon}{\partial y}\right)+\frac{\partial}{\partial z}\left(\frac{\mu_{\mathrm{T}}}{\sigma_\varepsilon}\frac{\partial \varepsilon}{\partial z}\right)+(C_1G-C_2\rho\varepsilon)\frac{\varepsilon}{k}, \tag{3}$$

where $G=\mu_{\mathrm{T}}\left[\left(\frac{\partial u}{L\partial y}\right)^2+\left(\frac{\partial u}{\partial z}\right)^2\right]$ and the dependence of μ_{T} on k and ε is given by the relation

$$\mu_{\mathrm{T}}=\frac{C_\mu\rho k^2}{\varepsilon}. \tag{4}$$

In (2)–(4) k and ε are the kinetic and dissipation of kinetic energy of turbulence, respectively, and $C_\mu, C_1, C_2, \sigma_k, \sigma_\varepsilon$ are the constants for $(k$–$\varepsilon)$-models that require further clarification for chemically reacting gases during the combustion of gas mixtures.

Let us choose the origin of the Cartesian coordinate system at the center of the initial section of the jet: the x axis is directed along the stream, and the y and z axes are parallel to the sides of a rectangular nozzle with side sizes 2a and 2b, respectively.

In numerical modeling of flows, the so-called simplified or parabolic Navier–Stokes equations are currently used, which are justified only in cases where the flow has a certain prevailing direction of motion, which includes jet flows. Parabolic models of flows of gas mixtures are based on the assumption of the presence of spatial anisotropy in the flow, expressed in a significant difference in the characteristic linear dimensions and velocities for different spatial directions [2].

To model the stated problem, we use parabolic systems of Navier–Stokes equations for multicomponent chemically reacting gas mixtures [2, 15, 16]. For the convenience of numerical solution, we reduce the system of equations to dimensionless form, choosing the following as the scale: for lengths we take the width of the nozzle side b; for speed, u_2 (hereinafter, index 2 refers to the initial values of combustible (main)); for density, ρ_2; for pressure, $\rho_2u_2^2$; for the total enthalpy and heat of formation of ith components, u_2^2; for effective turbulent viscosity, $b\rho_2u_2^2$; for heat capacity at constant pressure, (R/M_1); for molecular weight, M_i (M_1 is the molecular weight of the oxidizer) and also transform the inlet cross-section of the nozzle into a square area using the formula $y=\bar{y}/L$ ($L=a/b$) (in what follows we omit the tilde over the dimensionless variable). We get

$$\frac{\partial\rho u}{\partial x}+\frac{1}{L}\frac{\partial\rho\vartheta}{\partial y}+\frac{\partial\rho\omega}{\partial z}=0, \tag{5}$$

$$\rho u\frac{\partial u}{\partial x}+\rho\vartheta\frac{\partial u}{L\partial y}+\rho\omega\frac{\partial u}{\partial z}=-\frac{\partial P}{\partial x}+\frac{1}{L^2}\frac{\partial}{\partial y}\left(\mu_{\mathrm{T}}\frac{\partial u}{\partial y}\right)+\frac{\partial}{\partial z}\left(\mu_{\mathrm{T}}\frac{\partial u}{\partial z}\right), \tag{6}$$

$$\begin{aligned}\rho u\frac{\partial \vartheta}{\partial x}+\rho\vartheta\frac{\partial \vartheta}{L\partial y}+\rho\omega\frac{\partial \vartheta}{\partial z}=&-\frac{\partial P}{L\partial y}+\frac{4}{3L^2}\frac{\partial}{\partial y}\left(\mu_{\mathrm{T}}\frac{\partial \vartheta}{\partial y}\right)+\frac{\partial}{\partial z}\left(\mu_{\mathrm{T}}\frac{\partial \vartheta}{\partial z}\right)\\&-\frac{2}{3L}\frac{\partial}{\partial y}\left(\mu_{\mathrm{T}}\frac{\partial \omega}{\partial z}\right)+\frac{1}{L}\frac{\partial}{\partial z}\left(\mu_{\mathrm{T}}\frac{\partial \omega}{\partial y}\right),\end{aligned} \tag{7}$$

$$\begin{aligned}\rho u\frac{\partial \omega}{\partial x}+\rho\vartheta\frac{\partial \omega}{L\partial y}+\rho\omega\frac{\partial \omega}{\partial z}=&-\frac{\partial P}{\partial z}+\frac{4}{3}\frac{\partial}{\partial z}\left(\mu_{\mathrm{T}}\frac{\partial \omega}{\partial z}\right)+\frac{1}{L^2}\frac{\partial}{\partial y}\left(\mu_{\mathrm{T}}\frac{\partial \omega}{\partial y}\right)\\&+\frac{1}{L}\frac{\partial}{\partial y}\left(\mu_{\mathrm{T}}\frac{\partial \vartheta}{\partial z}\right)-\frac{2}{3L}\frac{\partial}{\partial z}\left(\mu_{\mathrm{T}}\frac{\partial \vartheta}{\partial y}\right),\end{aligned} \tag{8}$$

$$\rho u\frac{\partial H}{\partial x}+\rho\vartheta\frac{\partial H}{L\partial y}+\rho\omega\frac{\partial H}{\partial z}=\frac{1}{L^2Pr_{\mathrm{T}}}\frac{\partial}{\partial y}\left(\mu_{\mathrm{T}}\frac{\partial H}{\partial y}\right)+\frac{1}{Pr_{\mathrm{T}}}\frac{\partial}{\partial z}\left(\mu_{\mathrm{T}}\frac{\partial H}{\partial z}\right)$$
$$+\left(1-\frac{1}{Pr_{\mathrm{T}}}\right)\left[\frac{1}{L^2}\frac{\partial}{\partial y}\left(\mu_{\mathrm{T}}u\frac{\partial u}{\partial y}\right)+\frac{\partial}{\partial z}\left(\mu_{\mathrm{T}}u\frac{\partial u}{\partial z}\right)+\frac{\partial}{\partial z}\left(\mu_{\mathrm{T}}\vartheta\frac{\partial\vartheta}{\partial z}\right)+\frac{1}{L^2}\frac{\partial}{\partial y}\left(\mu_{\mathrm{T}}\omega\frac{\partial\vartheta}{\partial y}\right)\right]$$
$$+\left(\frac{4}{3}-\frac{1}{Pr_{\mathrm{T}}}\right)\left[\frac{1}{L^2}\frac{\partial}{\partial y}\left(\mu_{\mathrm{T}}\vartheta\frac{\partial\vartheta}{\partial y}\right)+\frac{\partial}{\partial z}\left(\mu_{\mathrm{T}}\omega\frac{\partial\omega}{\partial z}\right)\right]-\frac{1}{L}\frac{\partial}{\partial y}\left(\frac{2}{3}\mu_{\mathrm{T}}\vartheta\frac{\partial\omega}{\partial z}+\frac{1}{L}\frac{\partial}{\partial z}\left(\mu_{\mathrm{T}}\vartheta\frac{\partial\omega}{\partial y}\right)\right.$$
$$\left.+\frac{1}{L}\frac{\partial}{\partial y}\left(\mu_{\mathrm{T}}\omega\frac{\partial\vartheta}{\partial z}\right)-\frac{1}{L}\frac{\partial}{\partial z}\left(\frac{2}{3}\mu_{\mathrm{T}}\omega\frac{\partial\vartheta}{\partial y}\right)\right), \tag{9}$$

$$\rho u\frac{\partial\overline{\overline{C}}}{\partial x}+\rho\vartheta\frac{\partial\overline{\overline{C}}}{L\partial y}+\rho\omega\frac{\partial\overline{\overline{C}}}{\partial z}=\frac{1}{L^2Sc_{\mathrm{T}}}\frac{\partial}{\partial y}\left(\mu_{\mathrm{T}}\frac{\partial\overline{\overline{C}}}{\partial y}\right)+\frac{1}{Sc_{\mathrm{T}}}\frac{\partial}{\partial z}\left(\mu_{\mathrm{T}}\frac{\partial\overline{\overline{C}}}{\partial z}\right), \tag{10}$$

$$P=\rho T\sum_{i=1}^{N}\frac{C_i}{M_i}, \tag{11}$$

$$H=C_pT+\frac{u^2+\vartheta^2+\omega^2}{2}+\sum_{i=1}^{N}C_ih_i^*. \tag{12}$$

Formulas (1)–(3) are also given in dimensionless form, choosing $u_2^2, u_2^3/b$ to be the scales for the kinetic energy of turbulence and its dissipation and $u_2^2/(R/M_1)$ for the temperature. In equations (1)–(12) all notations are generally accepted, and laminar viscosity is calculated as $\mu_1 = \mathrm{const}\cdot T^{0{,}64}$, where const is calculated taking into account the collision diameter, characteristic temperature, parameter of the potential function of intermolecular interaction, as well as the collision integral for momentum transfer [2], and l is the mixing path length, defined as $\sqrt{b^2(Ly)+b^2(z)}$.

The equation for the concentration (10) is written in the form of a conservative Schwab–Zeldovich function with respect to mass concentration of the ith terms to one for a four-component mixture [4].

The conservative function $\overline{\overline{C}}$ at the nozzle exit of the combustible is equal to one, and that in the oxidizer zone is zero.

2. BOUNDARY AND INITIAL CONDITIONS

For this formulation, the system of equations (1), (5)–(12), or (2)–(12) can be solved using the following dimensionless boundary conditions:

(1) $x = 0$:

$$0\le y\le 1,\quad 0\le z\le 1,$$
$$u=1,\ \ \vartheta=0,\ \ \omega=0,\ \ H=H_2,\ \ P=P_2,\ \ \overline{\overline{C}}=1,\ \ k=k_2,\ \ \varepsilon=\varepsilon_2;$$
$$1<y<y_{+\infty},\ \ 1<z<z_{+\infty},$$
$$u=u_1,\ \ \vartheta=0,\ \ \omega=0,\ \ H=H_1,\ \ P=P_1,\ \ \overline{\overline{C}}=0,\ \ k=k_1,\ \ \varepsilon=\varepsilon_1; \tag{13}$$

(2) $x > 0$:

$$z=0,\ \ 0<y<y_{+\infty};\ \ \omega=0,\ \ \frac{\partial f}{\partial z}=0\ \ (f=u,\vartheta,H,\overline{\overline{C}},k,\varepsilon);$$
$$y=0,\ \ 0<z<z_{+\infty};\ \ \vartheta=0,\ \ \frac{\partial f}{\partial y}=0\ \ (f=u,\omega,H,\overline{\overline{C}},k,\varepsilon);$$
$$z=0,\ \ y=0,\ \ \omega=0,\ \ \vartheta=0,\ \ \frac{\partial f}{\partial y}=\frac{\partial f}{\partial z}=0\ \ (f=u,H,\overline{\overline{C}},k,\varepsilon); \tag{14}$$
$$z\to z_{+\infty},\ \ y\to y_{+\infty};\ \ u=u_1,\ \ \vartheta=0,\ \ \omega=0,\ \ H=H_1,\ \ P=P_1,\ \ \overline{\overline{C}}=0,\ \ k=k_1,\ \ \varepsilon=\varepsilon_1.$$

Here, the subscripts 1, 2, and ∞ denote the dimensionless quantities of the oxidizer and the combustible jet, respectively, as well as their values at infinity.

3. SOLUTION METHOD

The system of parabolic Navier–Stokes equations (5)–(9) is obtained by simply removing from the stationary Navier–Stokes equations all terms containing partial derivatives in the longitudinal direction.

Methods and algorithms for solving three-dimensional parabolic equations known from the literature were obtained according to the segregated method proposed in [15, 17] and implemented in the SIMPLE procedure.

In [17], parabolic procedures for three-dimensional internal flows are generalized in detail.

The main feature of the three-dimensional parabolic model is the separation of terms with pressure gradients in the longitudinal and transverse directions. In the case of internal flows, the pressure gradient in the direction of the main flow is determined from the condition of constant mass flow in each section plane.

The basic elements of this procedure can be used in the calculation of three-dimensional free jet flows, the pressure gradient in the longitudinal direction can be neglected or is known in advance. This situation occurs when a subsonic free jet flows through a rectangular nozzle with a finite aspect ratio into a cocurrent or submerged flow. As is known, the shape of such a jet in the cross section gradually changes in the longitudinal direction and finally becomes circular [7, 10]. In such flows, the assumption of neglecting the longitudinal pressure gradient and its small changes in the transverse plane is justified, which sometimes makes it possible to carry out calculations without taking into account pressure, i.e., a given pressure.

Next, we present a method and algorithm for calculating the problem posed with a given and variable pressure using spatial coordinates.

To numerically solve the system of equations (1), (5)–(12), and (2)–(12) with initial and boundary conditions (13), (14), we use a spatial two-layer decimal implicit finite-difference scheme. The region under consideration is covered with a grid $x = k_x i\Delta x$, $y = j\Delta y$, $z = k\Delta z$. Indices i, j, k denote the node numbers along the coordinate axes x, y, z; Nx, Ny, Nz are the numbers of points along the Ox, Oy, Oz axes, respectively; k_x is the coefficient of condensation of the calculated point along the axis Ox. Individual terms of the differentials were approximated with an order of accuracy $O(\Delta x, \Delta y^2, \Delta z^2)$. The solution to difference equations is sought by moving from the plane corresponding to the $(i-1)$th step, in the plane corresponding to ith step along the marching coordinate.

Equation (2)–(10) are perfectly parabolic and their solution can be obtained using the marching procedure along the x, y, z axes for determining $u, \vartheta, \omega, H, k, \varepsilon, \overline{\overline{C}}$.

Solution for the ith plane should be found starting from the value $k = 1$ (usually, this value k corresponds to the plane of symmetry), which determines the solution for all j. As a result, for given i and k we find a solution on a line normal to the symmetry surface, with $y = 0$. After this the index k increases by one and the solutions are obtained in another column by k. In general, in the difference relations used, the values of the sought quantities on the $(i-1)$th and $(k-1)$th layers are known if, when using a parabolic system of equations, the values of some flow parameters at the cross section $(k+1)$ are known. For jet streams as values of the $(k+1)$th cross section, we can take oxidizer data (flooded or slipstream).

4. CALCULATION METHOD AND ALGORITHM WITH A GIVEN PRESSURE

(1) On each design plane YOZ, along the directional axis Ox we set the accepted pressure distribution; initially, we prescribe the values of the unknowns from the previous plane as first approximations of the unknowns of (S)-iterations (index $i = 1$ corresponds to the inlet conditions (12)): the difference equation of motion along the x axis is solved and $(u_p)_{ijk}$ is determined (on each new calculation plane along the x axis, the solution to the system of equations begins with $k = 2$, while $k = 1$ corresponds to the plane of symmetry); the difference equation of motion along the y axis is solved and $(\vartheta_p)_{ijk}$ is determined using the value $(u_p)_{ijk}$; the difference equation of motion along the z axis is solved and $(\omega_p)_{ijk}$ is found using the values $(u_p)_{ijk}$ and $(\vartheta_p)_{ijk}$ (the solution uses an implicit variable direction scheme).

(2) The obtained preliminary solutions $u_p, \vartheta_p, \omega_p$ do not satisfy the continuity equation [1, 15, 17] written in the difference form. Therefore, the supposedly redundant continuity equation (5) is used to calculate the mass imbalance at each calculated grid point (i, j, k). The obtained solutions u, ϑ, ω at the $(S+1)$th iteration are expressed as calculated estimates $(u_p, \vartheta_p, \omega_p)$ and corrections $(u_c, \vartheta_c, \omega_c)$:

$$u = u_p + u_c, \quad \vartheta = \vartheta_p + \vartheta_c, \quad \omega = \omega_p + \omega_c. \tag{15}$$

The following question arises: how can we define u_c, ϑ_c, and ω_c at each design point (i, j, k)? The corrected velocities (15) must satisfy the continuity equation (5):

$$\frac{\partial \rho(u_p + u_c)}{\partial x} + \frac{1}{L}\frac{\partial \rho(\vartheta_p + \vartheta_c)}{\partial y} + \frac{\partial \rho(\omega_p + \omega_c)}{\partial z} = 0. \tag{16}$$

The potential Φ can be defined as follows:

$$\rho u_c = \frac{\partial \Phi}{\partial x}, \quad \rho \vartheta_c = \frac{\partial \Phi}{L \partial y}, \quad \rho \omega_c = \frac{\partial \Phi}{\partial z}. \tag{17}$$

We substitute (17) into (16) and obtain the Poisson equation

$$\begin{gathered} \frac{\partial^2 \Phi}{\partial x^2} + \frac{\partial^2 \Phi}{\partial y^2} + \frac{\partial^2 \Phi}{\partial z^2} = Q_p, \\ Q_p = -\left(\frac{\partial \rho u_p}{\partial x} + \frac{1}{L}\frac{\partial \rho \vartheta_p}{\partial y} + \frac{\partial \rho \omega_p}{\partial z} \right), \end{gathered} \tag{18}$$

where Q is the source term. The necessary corrections to velocity (15) can be numerically calculated from the distribution Φ, obtained from the difference equation (18) in the transverse plane. The difference algebraic equation can be written for the potential Φ at each grid point across the flow in the plane along i. Thus, we have a tridiagonal system of equations, provided that the values are known

$$\Phi_{i,j,k-1}, \quad \Phi_{i,j,k+1}, \quad \Phi_{i+1,j,k}, \quad \Phi_{i-1,j,k}.$$

The Poisson difference equation (18) is solved under the following basic assumptions.

(a) $\Phi_{i,j,k-1} = 0$, $\Phi_{i-1,j,k} = 0$, where velocity corrections are zero both in the $(i-1)$th plane and in the $(k-1)$th cross-section; here, conservation of mass is already ensured.

(b) $\Phi_{i,j,k+1} = 0$, $\Phi_{i+1,j,k} = 0$, where velocity corrections are zero both in the $(i+1)$th plane and in the $(k+1)$th cross-section, when their convergence is achieved in this plane and in the $(k+1)$th cross-section, respectively. These assumptions make it possible to reduce the system of algebraic equations to the tridiagonal system for Φ:

$$\Phi_{i,j-1,k} - 2\left(\left(\frac{\Delta y}{\Delta x}\right)^2 + 1 - \left(\frac{\Delta y}{\Delta z}\right)^2 \right)\Phi_{i,j,k} + \Phi_{i,j+1,k} = \Delta y^2 Q_{pi,j,k}. \tag{19}$$

The boundary conditions necessary to solve system (19) are chosen so that they are compatible with the specified boundary conditions for velocity (14). From the last line of the boundary condition (14) it is known that, if the velocities of the external flow are known in advance, then the function Φ at this boundary are zero:

$$\Phi_{i,Ny+1,k} = 0. \tag{20}$$

On the plane of symmetry at $y = 0$, $0 < z < z_{(+\infty)}$, in order for the last two lines of condition (13) to be fulfilled, the condition must be met:

$$\Phi_{i,1,k} = \Phi_{i,2,k}. \tag{21}$$

After this, by virtue of (21) and (20), using a scalar sweep [13] over all j ($j = \overline{1, Ny}$) we find $\Phi_{i,j,k}$. Using the obtained $\Phi_{i,j,k}$, we determine the velocity corrections using the difference approximations of expression (17) in the form

$$(u_c)_{ijk} = \Phi_{ijk} / \left(\Delta x \rho_{ijk}^{(s)}\right),$$

$$(\omega_c)_{ijk} = \Phi_{ijk} / \left(\Delta z \rho_{ijk}^{(s)}\right), \tag{22}$$

$$(\vartheta_c)_{ijk} = (\Phi_{i,j+1,k} - \Phi_{i,j-1,k}) / \left(2L\Delta y \rho_{ijk}^{(s)}\right).$$

Now, the adjusted velocities satisfy the continuity equation at each point in the section (k) plane (i), but do not exactly satisfy the equation of motion and other equations of the system.

(3) Next, by the energy equation (9) we can find $H_{ijk}^{(s+1)}$, from relation (12) we find $T_{ijk}^{(s+1)}$, from the equation of state we determine $\rho_{ijk}^{(s+1)}$, and from the equation of concentration of functions we find $\tilde{\tilde{C}}$. If we consider a variant of the algebraic model, then from (1) we calculate the viscosity $\mu_{ijk}^{(s+1)}$. In other words, using new solutions $u, \vartheta, \omega, \rho$ from the finite-difference solution of equations (2), (3), we calculate $k_{ijk}^{(s+1)}$ and $\varepsilon_{ijk}^{(s+1)}$, and from relation (4) we determine the turbulent viscosity μ_T. When calculating the effective viscosity using formula (1), the values $b(Ly)$ and $b(z)$ are defined as $b(Ly) = LNy\Delta y$, $b(z) = Nz\Delta z$. The values of individual concentration components C_i are also calculated.

(4) Because it is not possible to simultaneously satisfy the equation of motion and continuity and other equations of the system, steps (1)–(3) are usually repeated with iteration in each cross-section before moving on to the next one.

The convergence of the iteration to find a solution to the system of equations for a fixed ith plane of the kth cross-section at $j = \overline{1, Ny}$ is checked by the condition

$$\left|F_{i,j,k}^{(s+1)} - F_{i,j,k}^{(s)}\right| \le \varepsilon_1 \quad (F = u, \vartheta, \omega, H), \tag{23}$$

where ε_1 is a small number characterizing the accuracy of the calculation.

If condition (23) is not satisfied, then the solution is averaged:

$$F_{i,j,k}^{(s)} = \left(F_{i,j,k}^{(s)} + F_{i,j,k}^{(s+1)}\right)/2 \quad (F = u, \vartheta, \omega, H, \rho, k, \varepsilon),$$

and these solutions are perceived as the values of the previous sth iteration, and the calculation process is repeated from the first step. Otherwise, the condition is checked

$$\max_k \left|F_{i,j,k}^{(s+1)} - F_{\text{ext}}\right| > \varepsilon_2, \tag{24}$$

where ε_2 is a small number and F may be the value of the desired variables u, H. If this condition is met, then the number of calculated points along the y axis increases by one calculated point according to the recurrence relation $Ny = Ny + 1$, which characterizes the growth of the computational domain, i.e., the propagation of the jet boundary along the y axis, and, again, the calculations continue from the first step. If conditions (24) are not met, then it is considered that the solution to the system of equations on the ith plane in the kth cross-section has been found.

The condition for growing the calculation area along the OZ axis is checked

$$\max_j \left|F_{i,j,k}^{(s+1)} - F_{\text{ext}}\right| > \varepsilon_3, \tag{25}$$

where ε_3 is a small positive number.

If this condition is met, then the number of design points along the Z axis increases by one calculated point according to the recursive relation $NZ = NZ + 1$ (the value k increases by one), then we move on to the $(k+1)$th cross-section and, again, continue the calculations from the first step. If condition (25) is not satisfied, then the solution on the ith plane is found and it is necessary to move to the next plane along

the longitudinal coordinate X. Before moving to the next calculation plane along the OX axis, the closure of the plume shape on the axis of symmetry is checked for the combustion problem, and, to calculate the free air jet, the tendency of the longitudinal velocity to the velocity of the cocurrent flow is tested. If these conditions are violated, the iteration process continues from the first step.

5. CALCULATION METHOD AND ALGORITHM WITH VARIABLE PRESSURE

The system of equations (5)–(10) is partially parabolic, so their elliptical effects manifest themselves through the pressure field.

The latter requires that the solution, which is obtained by sequentially moving from one cross-section to another in the longitudinal direction, is refined by iteration. The need to carry out calculations taking into account pressure for three-dimensional turbulent jets of reacting gases lies in the fact that in the area of contact of the jets they are accompanied by sharp changes in temperature (combustion), and this, as is known, significantly changes the pressure value.

On the other hand, numerical solutions of partially parabolic equations require the development of new effective methods, which is what this part of the work is devoted to.

In Eqs. (6)–(8), the pressure terms are approximated as follows:

$$\frac{\partial P}{\partial x} = \frac{P^{(s+1)}_{i,j,k} - P^{(s+1)}_{i-1,j,k}}{\Delta x} + O(\Delta x), \quad \frac{\partial P}{\partial y} = \frac{P^{(s+1)}_{i,j+1,k} - P^{(s+1)}_{i,j-1,k}}{2\Delta y} + O(\Delta y^2),$$
$$\frac{\partial P}{\partial z} = \frac{P^{(s+1)}_{i,j,k+1} - P^{(s+1)}_{i,j,k-1}}{2\Delta z} + O(\Delta z^2). \tag{26}$$

Next, we present modifications of the SIMPLE method, a semi-implicit method for pressure-coupled equations [17, 18] for solving subsonic three-dimensional parabolic Navier–Stokes equations.

The proposed method is based on a cyclic sequence of prediction–correction operations for solving the equations.

The question is how to use the equations of motion and continuity to find the correct pressure distribution.

5.1. Method and Algorithm

(1) The first step is similar to the method in Section 4.

(2) We express true solutions u, ϑ, ω, and P, accordingly, as the found calculated (or intermediate) $P_p, u_p, \vartheta_p, \omega_p$ plus corrections $P_c, u_c, \vartheta_c, \omega_c$ as

$$P = P_p + \alpha_1 P_c, \tag{27}$$

$$u = u_p + u_c, \quad \vartheta = \vartheta_p + \vartheta_c, \quad \omega = \omega_p + \omega_c, \tag{28}$$

where α_1 is the relaxation parameter.

The velocity corrections are assumed to be determined by the pressure corrections according to very approximate three equations of motion in which the longitudinal convective terms are counterbalanced only by the pressure terms:

$$\rho u \frac{\partial u_c}{\partial x} = -\frac{\partial P_c}{\partial x}, \tag{29}$$

$$\rho u \frac{\partial \vartheta_c}{\partial x} = -\frac{1}{L}\frac{\partial P_c}{\partial y}, \tag{30}$$

$$\rho u \frac{\partial \omega_c}{\partial x} = -\frac{\partial P_c}{\partial z}. \tag{31}$$

Here, P_c can be considered some potential function (similar to Φ), which is used to generate velocity corrections that satisfy the continuity equation.

Applying difference analogs of differentials in the left-hand side of Eqs. (29)–(31), we obtain

$$(\rho u)_{ijk}^{(s)}\frac{(u_c)_{ijk}-(u_c)_{i-1,j,k}}{\Delta x}=-\frac{\partial P_c}{\partial x},$$
$$(\rho u)_{ijk}^{(s)}\frac{(\vartheta_c)_{ijk}-(\vartheta_c)_{i-1,j,k}}{\Delta x}=-\frac{\partial P_c}{L\partial y},$$
$$(\rho u)_{ijk}^{(s)}\frac{(\omega_c)_{ijk}-(\omega_c)_{i-1,j,k}}{\Delta x}=-\frac{\partial P_c}{\partial z},$$

and, under the assumption that the velocity corrections are zero in the $(i-1)$th plane along the longitudinal coordinate (conservation of mass is already ensured), the following can easily be obtained:

$$u_c=-\frac{\Delta x}{\rho u}\frac{\partial P_c}{\partial x},\quad \vartheta_c=-\frac{\Delta x}{L\rho u}\frac{\partial P_c}{\partial y},\quad \omega_c=-\frac{\Delta x}{\rho u}\frac{\partial P_c}{\partial z}. \tag{32}$$

The corrected velocities (28) must satisfy the continuity equation (5), taking into account (32) and assuming that u_p is a locally constant at each calculated grid point, we obtain the Poisson equation for P_c:

$$\begin{gathered}\frac{\partial^2 P_c}{\partial x^2}+\frac{1}{L^2}\frac{\partial^2 P_c}{\partial y^2}+\frac{\partial^2 P_c}{\partial z^2}=Q_p,\\ Q_p=\frac{u_p}{\Delta x}\left(\frac{\partial \rho u_p}{\partial x}+\frac{1}{L}\frac{\partial \rho \vartheta_p}{\partial y}+\frac{\partial \rho \omega_p}{\partial z}\right).\end{gathered} \tag{33}$$

Here, Q_p is the source term. To solve Eq. (33) numerically, we proceed to the difference equations; the algebraic equation can be written for the potential P_c at each grid point across the flow, these equations can be easily solved by introducing an educated guess as in assumptions (a) and (b) in Section 4.

These assumptions allow us to present a system of algebraic equations

$$\frac{1}{L^2}(P_c)_{i,j-1,k}+2\left[-\left(\frac{\Delta y}{\Delta x}\right)^2-\frac{1}{L^2}-\left(\frac{\Delta y}{\Delta z}\right)^2\right](P_c)_{i,j,k}+\frac{1}{L^2}(P_c)_{i,j+1,k}=(Q_p)_{i,j,k} \tag{34}$$

to solving a tridiagonal system for P_c.

The boundary conditions required to solve the system of equations (34) are chosen so that they are compatible with the specified boundary conditions for velocity and pressure.

As can be seen from the last line in (14), the velocity values u,ϑ,ω and the pressures are specified or they are known in advance (from the external concurrent flow); in this case u_c,ϑ_c,ω_c, and P_c are zero on this boundary:

$$(P_c)_{i,Ny+1,k}=0. \tag{35}$$

On the plane of symmetry, i.e., at $y=0$, $0<z<z_{+\infty}$, in order for the second line of condition (14) to be fulfilled, the condition must hold:

$$(P_c)_{i,1,k}=(P_c)_{i,2,k}. \tag{36}$$

Now, according to (35) and (36), using a scalar sweep over all j ($j=\overline{1,Ny}$), we find $(P_c)_{i,j,k}$. After finding $(P_c)_{i,j,k}$, we determine velocity and pressure corrections using difference approximations of expressions (32) taking into account assumptions (a) and (b) of Section 4 (P_c as Φ) and have

$$\begin{gathered}(u_c)_{i,j,k}=-\frac{(P_c)_{i,j,k}}{(\rho u_p)_{i,j,k}},\quad (\vartheta_c)_{i,j,k}=-\frac{(P_c)_{i,j+1,k}-(P_c)_{i,j-1,k}}{2L(\rho u_p)_{i,j,k}}\frac{\Delta x}{\Delta y},\\ (\omega_c)_{i,j,k}=-\frac{(P_c)_{i,j,k}}{(\rho u_p)_{i,j,k}}\frac{\Delta x}{\Delta z}.\end{gathered} \tag{37}$$

Using (37) and the values $(P_c)_{i,j,k}$ and employing expressions (27) and (28), we calculate the corrected pressure and velocities. These corrected velocities satisfy the continuity equation at each point in the

*k*th section in the *i*th plane, but do not exactly satisfy the equation of motion and other equations of the system (5)–(10), (2)–(3) until convergence is achieved.

The remaining calculation steps are similar to steps (3) and (4) given in Section 4.

5.2. Methodical Calculations

The described method and solution algorithm were implemented in the form of programs for modern personal computers. Using this program, calculations can be carried out for both laminar and turbulent three-dimensional jet flows, as well as internal flows.

To check the reliability of the numerical results using the developed method, the outflow of an air jet flowing from a rectangular nozzle with aspect ratios (1; 1), (1; 2), (1; 3), and (1; 4), borrowed from work [6].

First, convergence over spatial steps was checked in the following variants:

$$\Delta x = \Delta y = \Delta z = 0.1, \quad \Delta x = \Delta y = \Delta z = 0.05, \quad \Delta x = \Delta y = \Delta z = 0.01.$$

Serial numerical calculations have shown that it is better to carry out calculations with the second option, the results of which differ from the third by 2–3%, and at the same time saving computer calculation time. It turns out that computer calculation time is saved much more if you perform calculations with a variable step (with selection k_x). Here and further, in all calculations Δx varied from 0.01 to 0.25, and at the same time in the initial participation the step did not exceed the value of 0.05.

The second methodological study was the growing (propagation) of the boundary of the computational domain using two approaches:

(1) according to conditions (24) and (25) (small numbers $\varepsilon_1 = \varepsilon_2 = \varepsilon_3 = 5\times10^{-4}$);

(2) carrying out calculations for a sufficiently large number of design points along the longitudinal section, i.e., $Nz \times Ny = 300 \times 300$.

Numerical experiments carried out in two versions showed that the expansion of the jet is only three to four points greater compared to the first approach, but the first is much more acceptable due to the savings in computational time.

It is necessary to emphasize the usefulness of the sequence of using intermediate (iterative) solutions for solving spatial problems of aerohydrodynamics of heat and mass transfer. For these purposes, numerical experiments were carried out:

—with prescribed first approximations $F_{i,j,k}^{(s)}$ ($F = u, \vartheta, \omega, \rho, H$) we determined $F_{i,j,k}^{(s+1)}$;

—the approach given in the method of Section 4, i.e., for each global iteration, each new value of the unknown is used to find the next one, showed its advantages over the first in that, sometimes, it turned out to be economical until the fifth or sixth iteration.

Comparisons of the calculated data with the experimental results of work [6] were carried out on the distribution of the pulse flux density in different cross-sections of the jet for a nozzle with the nozzle aspect ratio (1; 1), (1; 2), (1; 3), and (1; 4); they agree well.

The small difference in the results can be explained by the fact that during the experiments it was assumed that the transverse components of the velocity are nonzero in the initial section, and in our case the calculations were carried out with zero transverse velocities.

For a nozzle with an aspect ratio (1; 1), from the very beginning the jet area expansion in the direction of the Z axis decreases, while in the direction of the Y axis it grows [10, 17–20], i.e., at the beginning the jet transforms into an ellipse shape, and, then, as the flow moves downward, the shape of the jet takes on a circular shape, which is confirmed by the experimental data of the authors of [10, 17–20]. Figure 1 present velocity profiles ω along the y ($z = 0$) axis showing that the values ω, ϑ become comparable in magnitude with the value of the longitudinal velocity in the initial sections of the jet at the boundary of the displacement zone, and, when moving away from the nozzle exit, the maximum value of the velocity ω, ϑ

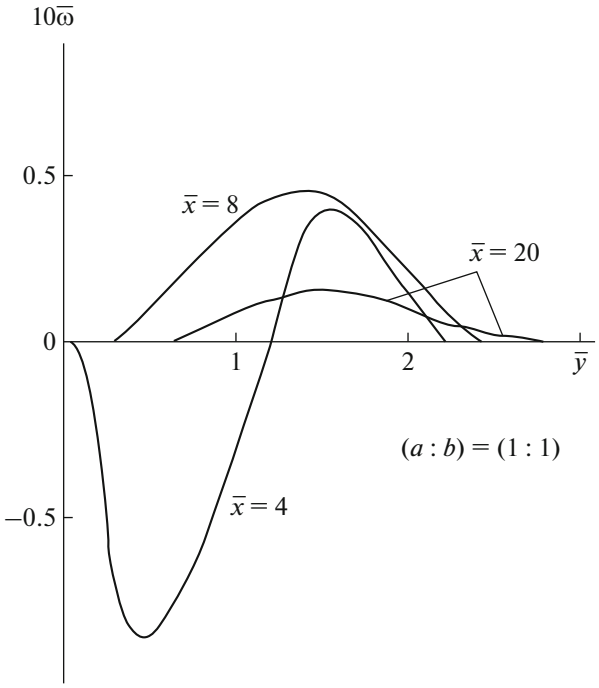

Fig. 1. Transverse speed distribution ω in different cross-sections of the jet along the axis y ($z = 0$).

tends to zero, i.e., the jet then behaves as a direct flow and can be considered an axisymmetric problem. The above studies are for a nozzle with a size of 20 mm × 20 mm (see [6]) at $P_1 = P_2 = 1$ atm, $u_2 = 38$ m/s, $u_1 = 0$ and $T_1 = T_2 = 300$ K based on the algebraic model of turbulence (1) at $\alpha = 0.5$, $\varkappa = 0.01$, $\mu_1 \neq 0$.

Similar studies were carried out on the basis of a two-parameter turbulence model (2)–(4).

In the calculations, the dimensionless initial values of the kinetic energy of jet turbulence vary from 0.001 to 0.1 of the longitudinal velocity, and the dissipation of turbulence energy $\varepsilon = 0.005$. To avoid dividing by zero, the initial values of resting air k and ε remain constant and equal to 0.005 and 0.00001, respectively.

Figures 2a and 2b show the longitudinal velocity profiles in different cross sections of the jet and a comparison of the calculated data obtained on the basis of the algebraic model and k–ε-turbulence models in different initial values k.

From the results it is clear that at small values k the core of the jet is noticeably preserved.

In the initial sections of the jet, the results of model calculations are in good agreement with experimental data (because the results based on the algebraic model were in good agreement with the experimental data of [6]); further, with distance from the channel exit, the results based on the (k–ε)-turbulence models are underestimated.

Satisfactorily matching results were obtained after numerous trial calculations using selected empirical constants (models (2)–(4)), the values of which became equal: $C_\mu = 0.08$, $C_1 = 1.3$, $C_2 = 1.5$, $\sigma_k = 1$, $\sigma_\varepsilon = 1.3$.

The results, as well as the first moment models, indicate that the width of the jet in the direction of the major axis of the hole initially decreases, while in the direction of the minor axis it increases. At some distance downstream, their values become equal, after which both axial widths y and z increase almost equally, i.e., the jet turns into a circular one ($\bar{x} = 5$). Apparently, the initial decrease in the width of the jet is most likely associated with the presence of lateral velocities.

The saddle-shaped behavior of the longitudinal velocity profiles in the direction of the major axis (Fig. 2b) was observed in the experiments of Sforza [20], but was not obtained numerically using the k–ε-model in [19], where a three-dimensional turbulent free jet flowing from a rectangular nozzle was studied.

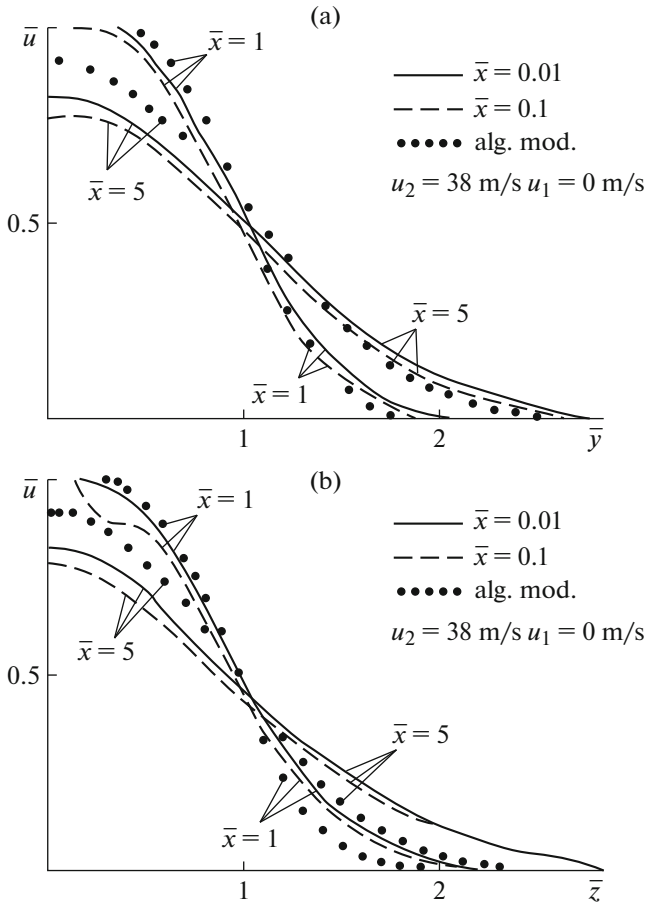

Fig. 2. Comparison of calculation results within the framework of algebraic and (k–ε)-turbulence models longitudinal velocity profiles along the (a) y and (b) z axes.

The numerical result, which cannot be obtained in calculations by the authors of [19], even when modifying the initial conditions, can be explained by the fact that additional flows caused by turbulence can contribute to the transfer of fluid with a high momentum from the central part of the jet to the edges, such thus leading to the formation of saddle-shaped velocity profiles.

5.3. Application of the Proposed Methods for the Numerical Study of Three-Dimensional Turbulent Reacting Jets to the Calculation of a Three-Dimensional Turbulent Plume in a Submerged Air Flow

Below are some results of a numerical study of three-dimensional turbulent diffusion combustion of a propane–butane mixture flowing from a square nozzle and propagating into a quiescent medium of air (oxidizer). It is assumed that the velocities, temperatures, and concentrations of the jets and the medium were set to be uniform and stepped at the nozzle exit, and the pressure of the jet and the medium were identical to each other and equal to atmospheric pressure, i.e., $P_1 = P_2 = P_{\text{atm.}}$.

For the calculation version, the initial parameter values were used from [21].

(1) The parameters of the oxidizer zone are as follows:

$$T_1 = 300 \text{ K}, \quad u_1 = 0, \quad (C_1)_1 = 0.232, \quad (C_2)_1 = 0, \quad (C_3)_1 = 0, \quad (C_4)_1 = 0.768$$

(if the (k–ε)-model is used, then $k_1 = \beta_1$, $\varepsilon_1 = \gamma_1$).

(2) The parameters of the fuel mixture have the form

$$T_2 = 1200 \text{ K}, \quad u_1 = 61 \text{ m/s}, \quad (C_1)_2 = 0, \quad (C_2)_2 = 0.12, \quad (C_3)_2 = 0, \quad (C_4)_2 = 0.88$$

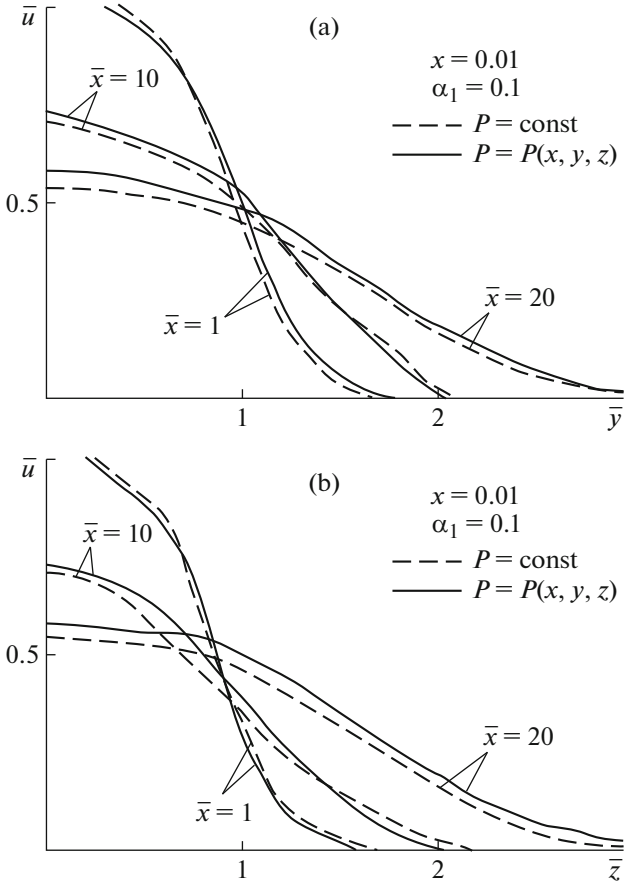

Fig. 3. Influence of the relaxation coefficient α_1 on the transverse distribution of longitudinal velocity along the (a) y and (b) z axes.

(if the (k–ε)-model is used, then $k_2 = \beta_2 u_2^2$, $\varepsilon_2 = \gamma_2 K_2^{3/2}$), where $\gamma_1, \gamma_2, \beta_1$ and β_2 are some dimensionless constants, and $\mathrm{Pr_T} = \mathrm{Sc_T} = 0.7$.

It can be noted that, when formulating the boundary conditions regarding the kinetic energy of turbulence, experimental materials from existing sources were used [22, 23], and, regarding the dissipation of the kinetic energy of turbulence, the boundary values were taken intuitively during a numerical experiment, i.e., by varying the values of the constants $\gamma_1, \gamma_2, \beta_1$, and β_2.

Thus, in the calculations β_2 varied so that the dimensionless initial value of the kinetic energy of turbulence did not exceed 10% of the dimensionless initial velocity of the fuel jet.

Below, we present some numerical results and their comparisons obtained on the basis of the algebraic model ($\varkappa = 0.01$, $\alpha = 0.5$) at constant and variable pressure, as well as on the basis of the (k–ε)-turbulence models ($\overline{k} = 0.01$, $\overline{k} = 0.05$, $C_\mu = 0.08$, $C_1 = 1.3$, $C_2 = 1.5$, $\sigma_k = 1$, $\sigma_\varepsilon = 1.3$) at constant pressure.

Numerical results showed that, with successful selection $\varkappa$ ($\varkappa = 0.01$) and initial turbulent energy k_2 ($\overline{k_2} = 0.01$) with an isobaric process, it is possible to obtain good agreement between the results in the initial sections of the XOY and XOZ planes.

Distributions of the axial value of the longitudinal velocity calculated based on the (k–ε)-turbulence model and based on the algebraic model of turbulence on the axis of symmetry of the flow, differ little.

It can be noted, when it is necessary to obtain only the parameters of the averaged flow, that there is no need to involve multiparameter turbulence models, but it is quite sufficient to use simple expressions for exchanging the coefficient of turbulent viscosity (1).

The use of an algebraic model of turbulence is convenient for practical purposes of engineering analysis, and the use of higher-order turbulence models in a number of cases allows us to get closer to under-

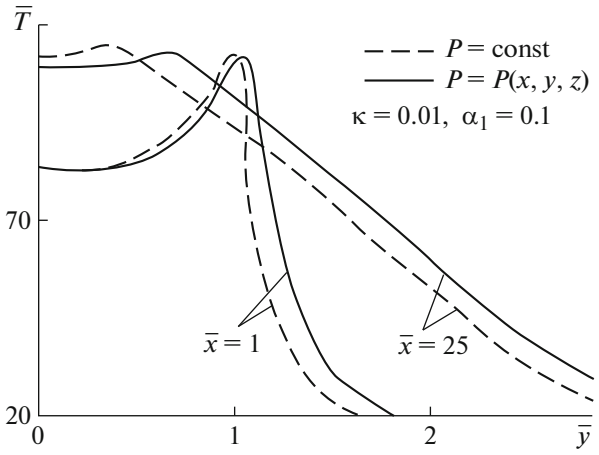

Fig. 4. Comparison of the temperature distribution of isobaric and nonisobaric jets.

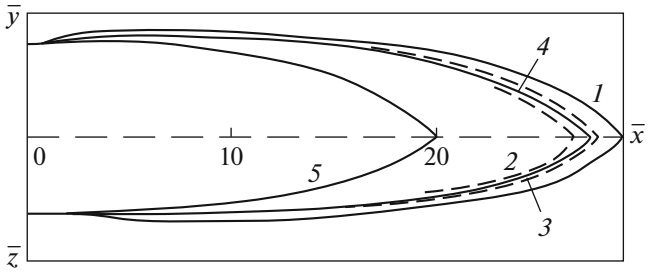

Fig. 5. Effect of pressure gradient on plume shape: (*1*) $P = P(x, y, z)$, $\alpha_1 = 0.1$; (*2*) and (*3*) $(k - \varepsilon)$-turbulence model at $k_2 = 0.05$ and $k_1 = 0.01$; and (*4*) and (*5*) algebraic model for $\varkappa = 0.01$ and $\varkappa = 0.1$.

standing of those physical phenomena that determine the detailed structure of physical and chemical processes in three-dimensional turbulent reacting jets.

Figures 3a and 3b show the distribution of longitudinal velocity at different cross-sections along the longitudinal coordinate at constant (dashed line) and variable (solid line, $\alpha_1 = 0.1$) pressures.

It is clear from the graphs that pressure variability noticeably affects the velocity (and temperature) profiles in the initial sections of the jet, and, when moving away from the nozzle exit, the influence of pressure can be considered insignificant, because the considered jets of reacting gases propagating in free space and pressure quickly tend to a constant value. It should be noted that deformation of the longitudinal velocity profiles is observed in the initial cross-sections of the jet along the y and z axes in both versions, i.e., when calculating with and without pressure. Figure 4 shows the temperature distribution at different cross-sections of isobaric ($P = \text{const}$) and nonisobaric ($P = P(x, y, z)$, $\alpha_1 = 0.1$) jets. Analyzing these graphs, we can conclude that taking into account the pressure gradient does not significantly affect the maximum value of the plume temperature.

Figure 5 shows the configurations of the diffusion plume for comparison.

From the shape of the plumes it is clear that the decrease in κ and $\overline{k_2}$ at constant pressure and at variable pressure $\alpha_1 = 0.1$ leads to a significant increase in the plume length. Numerical results showed that, taking into account the variability and constancy of pressure, the length of the plume in the first option is higher, but the pressure variability does not significantly affect the configuration of the plume.

FUNDING

This work was supported by ongoing institutional funding. No additional grants to carry out or direct this particular research were obtained.

CONFLICT OF INTEREST

The author of this work declares that he has no conflicts of interest.

REFERENCES

1. E. S. Oran and J. P. Boris, *Numerical Simulation of Reactive Flow* (Elsevier, 1987).
2. Yu. V. Lapin and M. Kh. Strelets, *Internal Flows of Gas Mixtures* (Nauka, Moscow, 1989).
3. V. R. Kuznetsov and V. A. Sabel'nikov, *Turbulence and Combustion* (Nauka, Moscow, 1986).
4. I. K. Khuzhaev and M. M. Khamdamov, *Numerical Algorithms for Calculating Turbulent Jet Flows of Reacting Gases* (Durdona, Bukhara, Uzbekistan, 2022).
5. H. H. Fernholz and E. Krause, *Three-Dimensional Turbulent Boundary Layers: Proceedings of the Symposium* (Springer, Berlin, 1982).
6. I. B. Palatnik and D. Zh. Temirabaev, "On propagation of free turbulent jets flowing from a rectangular nozzle," Probl. Teploenergetiki Prikl. Teplofiz., No. 1, 18–22 (1964).
7. S. I. Isataev, G. Toleuov, and M. S. Isataev, "Studying the average characteristics of three-dimensional turbulent jets," Vestn. Kazakhskogo Nats. Univ. Ser. Fiz., No. 2, 54–60 (2012).
8. M. A. Laryushkin, "Some regularities of the effect of initial level of turbulence on the development of a rectangular jet," Tr. Mosk. Energ. Inst. **524**, 26–36 (1981).
9. M. Nikjooy, K. C. Karki, and H. C. Mongia, "Calculation of turbulent three-dimensional jet-induced flow in a rectangular enclosure," in *28th Aerospace Sciences Meeting* (American Institute of Aeronautics and Astronautics, 1991), pp. AIAA 1990–684.
https://doi.org/10.2514/6.1990-684
10. K. Kuzov, "Aerodynamics of jets flowing from rectangular nozzles," Prom. Teplotekh. **12** (4), 38–44 (1990).
11. N. Trentacoste and P. Sforza, "Further experimental results for three-dimensional free jets," AIAA J. **5**, 885–891 (1967).
https://doi.org/10.2514/3.4096
12. Yu. P. Golovachev, A. I. Zhmakin, and A. A. Shmidt, "Numerical solution to some problems of physical dynamics," in *Problems of Fluid and Gas Dynamics* (Izd-vo S.-Peterb. Gos. Tekh. Univ., St. Petersburg, 2000), pp. 153–179.
13. D. A. Anderson, J. C. Tannehill, and R. H. Pletcher, *Computational Fluid Mechanics and Heat Transfer* (McGraw-Hill, New York, 1984).
14. S. Khodzhiev, Sh. S. Iuldoshev, and Z. Z. Shirinov, "Numerical modeling of three-dimensional turbulent jets of reacting gases based on algebraic model," in *Modern Problems of Applied Mathematics and Information Technology: Proc. Int. Sci.-Pract. Conf.* (Bukhara, 2021), pp. 140–142.
15. S. Khodzhiev, "Method for calculating nonisobaric three-dimensional turbulent jets of reacting gases flowing from a rectangular nozzle," in *Topical Problems of Wave Propagation in Liquid Multiphase Mixtures and Various Media* (Fan, Tashkent, 1999), pp. 408–409.
16. S. V. Patankar and D. B. Spalding, "A calculation procedure for heat, mass and momentum transfer in three-dimensional parabolic flows," Int. J. Heat Mass Transfer **15**, 1787–1806 (1972).
https://doi.org/10.1016/0017-9310(72)90054-3
17. S. V. Patankar, *Numerical Heat Transfer and Fluid Flow*, Series in Computational Mehtods in Mechanics and Thermal Sciences (CRC Press, Boca Raton, Fla., 1980).
https://doi.org/10.1201/9781482234213
18. J. J. McGuirk and W. Rodi, "The calculation of three-dimensional turbulent free jets," in *Turbulent Shear Flows I*, Ed. by F. Durst, B. E. Launder, F. W. Schmidt, and J. H. Whitelaw (Springer, Berlin,), pp. 71–83.
https://doi.org/10.1007/978-3-642-46395-2_6
19. P. M. Sforza, M. H. Steiger, and N. Trentacoste, "Studies on three-dimensional viscous jets.," AIAA J. **4**, 800–806 (1966).
https://doi.org/10.2514/3.3549
20. L. A. Vulis and L. P. Yarin, *Aerodynamics of Plume* (Energiya, Leningrad, 1978).
21. A. Agulykov, K. E. Dzhaugashtin, and L. P. Yarin, "Structure of three-dimensional turbulent jets," Fluid Dyn. **10**, 884–889 (1975).
https://doi.org/10.1007/bf01023263
22. V. P. Dvoinishnikov, N. A. Laryushkin, and V. P. Knyaz'kov, "Effect of initial conditions on the development of turbulent jets," Energetika Transp., No. 4, 167–170 (1981).

Publisher's Note. Allerton Press remains neutral with regard to jurisdictional claims in published maps and institutional affiliations.